FRONTIERS OF PHYSICS

RESEARCH ARTICLE
Volume 21 / Issue 5 / 053201 / 2026

Transferring quantum entangled states of photonic qubits via a quantum switch

Wen-Hao Kong[1,*], Jia-Heng Ni[1,*], Yi-Hao Kang[1], Li Yu[1], Qi Zhang[1], Yu Zhang[2], Qi-Ping Su[1,†], Chui-Ping Yang[1,‡]

1 School of Physics, Hangzhou Normal University, Hangzhou 311121, China
2 School of Physics, Nanjing University, Nanjing 210093, China
*These two authors contributed equally to this work.
Corresponding authors. E-mail: †sqp@hznu.edu.cn, ‡yangcp@hznu.edu.cn
Received September 12, 2025; accepted December 11, 2025

ABSTRACT

The controlled transfer of quantum entangled states is a fascinating topic in quantum physics, and has potential applications in fields such as quantum network communication, distributed quantum information processing, and development of quantum functional devices. This study focuses on a circuit quantum electrodynamics (QED) system, comprising an input port, two output ports, and a quantum switch. The input port or each output port contains n microwave cavities. The switch is a superconducting transmon qutrit (three-level quantum system). The vacuum and single-photon states in each cavity encode a photonic qubit. We demonstrate that the single-excitation symmetric (SES) entangled state of n photonic qubits can be transferred from the n cavities at the input port to the n cavities at either of the two output ports, controlled by the switch. Remarkably, the operational time decreases as the number n increases. The only use of qutrit-cavity resonant interaction enables rapid quantum state transfer while effectively suppressing system decoherence. This proposal can be used to achieve the controlled transfer of both Bell states and W states of photonic qubits via a quantum switch. To validate the experimental feasibility, we numerically simulate two scenarios: (i) transferring the Bell state of two photonic qubits, and (ii) transferring the W state of three photonic qubits. This proposal may be extended to accomplish the same task in other physical systems, where the switch is implemented with a three-level artificial atom of different types while each cavity is a microwave or optical cavity.

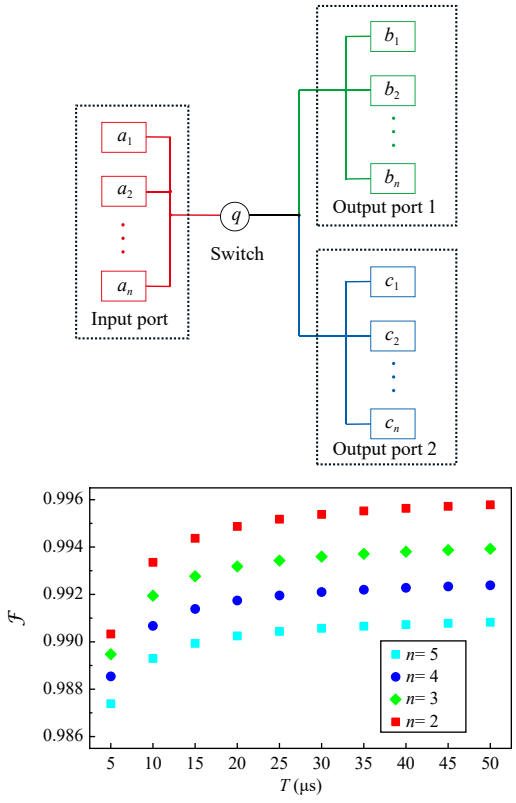

Keywords state transfer, photonic qubit, quantum switch, W state, circuit QED

1 Introduction and motivation

The new and rapidly growing field of circuit quantum electrodynamics (QED), consisting of superconducting (SC) artificial atoms and microwave cavities or resonators, offers extremely exciting prospects for quantum information processing (QIP) and quantum simulations on a chip [1]. In circuit-QED systems, SC artificial atoms can interact with microwave radiation fields in a more freely controlled and engineered manner [2–8].

Higher Education Press

https://doi.org/10.15302/frontphys.2026.053201

Experiments have achieved the strong-coupling or ultra-strong-coupling regime of a SC artificial atom with a microwave cavity (or resonator) [9–11]. SC artificial atoms can be fabricated using modern integrated circuit technology, their properties can be characterized and adjusted in situ, and their coherence time can reach from hundreds of microseconds [12–14] to even over 1 ms [15, 16]. Additionally, microwave cavities or resonators host microwave photons with lifetimes comparable to or longer than that of SC artificial atoms [17–19]. Therefore, both SC artificial atoms and microwave cavities have been utilized as the basic information processing units for implementing QIP. The rapid development and continuous progress have demonstrated the great potential of microwave superconducting circuit QED systems as multi-functional hardware architectures for the realization of QIP devices (for reviews, see Refs. [1, 5, 20–23]).

Transferring quantum states from one location to different locations is of fundamental interest in quantum physics, and has potential applications in fields such as networked quantum communication, distributed QIP, and development of quantum functional devices. A number of theoretical works have been devoted to realizing quantum state transfer between SC qubits (two-level quantum systems) [24–36]. Experimentally, much progress has been achieved in transferring quantum states between SC qubits. For instance, experiments have demonstrated: (i) the on-chip transfer of quantum states between two SC qubits coupled through a cavity [37, 38], a tunable coupler [39], or a tunable SC qubit [40], (ii) quantum state transfer between two SC qubits in a 4-qubit chain [39–43] or a six-qubit chain [44], (iii) the microwave-photon-mediated long-distance quantum state transfer between two SC qubits in different modules [45] or at different nodes in a network [46–49], and (iv) the phonon-mediated remote quantum state transfer between two SC qubits at different nodes of a network [50]. Furthermore, experiments have demonstrated the quantum state transfer between two SC qubits on a superconducting chip by utilizing standard teleportation protocols [51, 52]. More recently, deterministic quantum state teleportation between two SC qubits located at distant superconducting chips has been experimentally implemented [53]. Notably, the realization of quantum state transfer has also been investigated in other types of physical systems (e.g., see [54–58] and references therein).

On the other hand, there has been great interest in transferring quantum states between microwave cavities or bosonic systems. Numerous theoretical proposals have been put forward for realizing quantum state transfer between microwave cavities [59–64] or bosonic systems [65–67]. Moreover, experimental advances have been achieved in this fascinating field. For example, experiments have demonstrated the transfer of Fock and coherent states between remote microwave cavities or resonators connected by a transmission line [68, 69], the two-way transfer of single photons between two chips linked by a coaxial cable [70], and the transfer of quantum states between superconducting cavities without exchange interactions [71]. Additionally, experiments have implemented quantum state transfer of a photonic qubit, encoded using the vacuum and single-photon states, between two remote cavities linked by a coaxial cable [72].

In this work we consider a circuit-QED system, which consists of an input port, two output ports, and a quantum switch [Fig. 1(a)]. The input port and each output port contain n microwave cavities, respectively [Fig. 1(a)]. The switch is a transmon qutrit (three-level quantum system) [Fig. 1(a)]. For each cavity, its vacuum and single-photon states are utilized to encode a photonic qubit. We show that the single-excitation symmetric (SES) entangled state of n photonic qubits can be transferred from the n cavities at the input port to the n cavities at either of the two output ports, controlled by the switch.

As shown below, this proposal has these distinguishing features and advantages. First, the state transfer is simple because it requires only a four-step operation. Second, the operational time decreases as the number n of cavities (in the input port or each output port) increases. Third, since only qutrit-cavity resonant interactions are employed, the state transfer can be fast performed and thus decoherence from the system is greatly reduced. Last, since the SES entangled state is a W-type entangled state for $n \geq 3$ and a Bell entangled state for $n = 2$, this proposal can be used to transfer both W states and Bell states of photonic qubits via the control of a quantum switch.

As an example, we numerically analyze the experimental feasibility in two scenarios: transferring the Bell state of two photonic qubits from two cavities at the input port to two cavities at either of the two output ports, and transferring the W state of three photonic qubits from three cavities at the input port to three cavities at either of the two output ports, via the control of a quantum switch. This proposal may be extended to accomplish the same task in other physical systems, where the switch is implemented with a three-level artificial atom (e.g., a quantum dot, an NV center, a magnon, and a superconducting qutrit of different types), while each cavity is a microwave or optical cavity.

The novelties of our proposal can be highlighted as follows. (i) In contrast to previous works [24–74], where the quantum states are transferred from the input ports to fixed output ports, our work introduces a quantum-switch-controlled transfer of entangled states across multiple photonic qubits. This enables controlled routing for a superconducting quantum network. (ii) Different from the controlled transfers of a single-qubit state

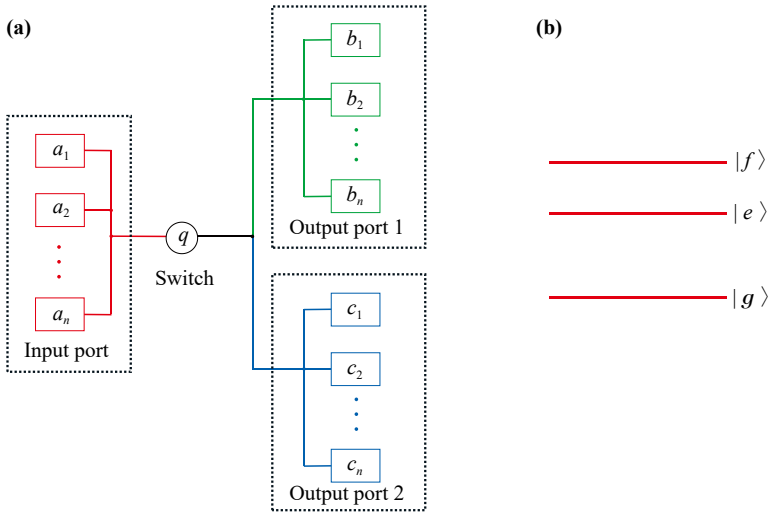

Fig. 1 **(a)** Schematic diagram for a circuit-QED system, which includes an input port, two output ports and a quantum switch. The switch is a SC transmon qutrit q, which is coupled to the n cavities $(a_1, a_2, \cdots, a_n)$ at the input port, the n cavities $(b_1, b_2, \cdots, b_n)$ at the output port 1, and the n cavities $(c_1, c_2, \cdots, c_n)$ at the output port 2. Each square represents a one-dimensional (1D) or three-dimensional (3D) microwave cavity, which is capacitively or inductively coupled to the qutrit q. **(b)** Level configuration of the transmon qutrit. The level spacings between the upper two levels is smaller than that between the two lowest levels.

[75–78], the present proposal enables direct controlled transfer of multi-qubit entangled states. (iii) In the present study, the operational time decreases with increasing qubit number, which increases the scalability advantage. The above-mentioned advantages make our proposal particularly suitable to transfer multi-qubit entangled states in an on-chip quantum networks where controlled state distribution is essential.

The rest of this paper is organized as follows. In Section 2, we will explicitly show how to realize the controlled transfer of the SES entangled state of n photonic qubits via a quantum switch. In Section 3, we will discuss the experimental feasibility of transferring the Bell state of two photonic qubits and the W state of three photonic qubits via the control of the switch. A concluding summary is presented in Section 4.

2 Implementing entangled state transfer via a quantum switch

Consider a circuit-QED system, which consists of one input port, two output ports (1,2), and a quantum switch [Fig. 1(a)]. The input port contains n identical microwave cavities $(a_1, a_2, \cdots, a_n)$ with frequency ω_a, the output port 1 contains n microwave cavities $(b_1, b_2, \cdots, b_n)$ with frequency ω_b, the output port 2 contains n microwave cavities $(c_1, c_2, \cdots, c_n)$ with frequency ω_c, and the quantum switch comprises a SC transmon qutrit. For the transmon qutrit, the three levels are labelled as $|g\rangle$, $|e\rangle$, and $|f\rangle$ [Fig. 1(b)].

Assume that, initially, the qutrit is in an arbitrary state $\alpha|g\rangle + \beta|e\rangle$ (with $|\alpha|^2 + |\beta|^2 = 1$), each cavity at the output ports is in the vacuum state $|0\rangle$, and the n cavities $(a_1, a_2, \cdots, a_n)$ at the input port are in the following SES entangled state

$$\begin{aligned}|SES\rangle_{a_1 a_2 \cdots a_n} = \frac{1}{\sqrt{n}}(&|00\cdots001\rangle_{a_1 a_2 \cdots a_n} \\ &+ |00\cdots010\rangle_{a_1 a_2 \cdots a_n} + \cdots \\ &+ |10\cdots000\rangle_{a_1 a_2 \cdots a_n}),\end{aligned} \tag{1}$$

where $|0\rangle_{a_j}$ and $|1\rangle_{a_j}$ are, respectively, the vacuum state and the single-photon state of cavity a_j $(j = 1, 2, \cdots, n)$. One can see that the SES entangled state in Eq. (1) is a complete-symmetry entangled state with a single-photon excitation in the n input cavities, and the single photon being occupied in each cavity with an equal probability. The initial state of the whole system is thus given by

$$|\psi(0)\rangle = |SES\rangle_{a_1 a_2 \cdots a_n} (\alpha|g\rangle_q + \beta|e\rangle_q) \prod_{j=1}^{n} |0\rangle_{b_j} \prod_{j=1}^{n} |0\rangle_{c_j}, \tag{2}$$

where $|0\rangle_{b_j}$ ($|0\rangle_{c_j}$) is the vacuum state of cavity b_j (c_j) with $j = 1, 2, \cdots, n$, and the subscript q represents the qutrit as mentioned above.

Suppose that the qutrit is initially decoupled from the cavity system [Fig. 2(a)]. The procedure for transferring the SES entangled state from the n cavities $(a_1, a_2, \cdots, a_n)$ to the n cavities $(b_1, b_2, \cdots, b_n)$ or the n cavities $(c_1, c_2, \cdots, c_n)$ via the control of the switch is as follows:

Step 1: Adjust the level spacings of the qutrit to

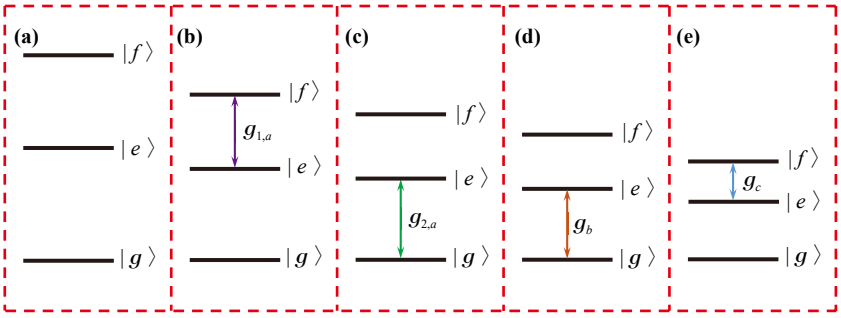

Fig. 2 Illustration of the level structure of the transmon qutrit before or during the state-transfer operation. **(a)** The level structure before the state-transfer operation, while **(b–e)** the change of the level structure during the state-transfer operation. In (a), the qutrit is decoupled from the cavity system. In (b), the n cavities $(a_1, a_2, \cdots, a_n)$ are resonant with the $|e\rangle \leftrightarrow |f\rangle$ transition of the qutrit with coupling constant $g_{1,a}$. In (c), the n cavities $(a_1, a_2, \cdots, a_n)$ are resonant with the $|g\rangle \leftrightarrow |e\rangle$ transition of the qutrit with coupling constant $g_{2,a}$. In (d), the n cavities $(b_1, b_2, \cdots, b_n)$ are resonant with the $|g\rangle \leftrightarrow |e\rangle$ transition of the qutrit with coupling constant g_b. In (e), the n cavities $(c_1, c_2, \cdots, c_n)$ are resonant with the $|e\rangle \leftrightarrow |f\rangle$ transition of the qutrit with coupling constant g_c.

have its $|e\rangle \leftrightarrow |f\rangle$ transition resonant with the n cavities $(a_1, a_2, \cdots, a_n)$ [Fig. 2(b)]. In the interaction picture and after applying the rotating-wave approximation (RWA), the Hamiltonian is given by (assuming $\hbar = 1$)

$$H_1 = g_{1,a} \sum_{j=1}^{n} \hat{a}_j |f\rangle_q \langle e| + \text{h.c.}, \tag{3}$$

where $\hat{a}_j$ is the photon annihilation operator of cavity a_j $(j = 1, 2, \cdots, n)$, and $g_{1,a}$ is the coupling constant between each of the cavities $(a_1, a_2, \cdots, a_n)$ and the $|e\rangle \leftrightarrow |f\rangle$ transition of the qutrit. In circuit QED, the cavity-qutrit coupling reaches strong or ultra-strong regimes. The physical unit of the coupling constant is usually MHz. Here and below, the "h.c." means "Hermitian conjugate terms". It is straightforward to show that under the Hamiltonian (3), one has the following state transformation

$$\begin{aligned} |SES\rangle_{a_1 a_2 \cdots a_n} |e\rangle_q \to \cos\left(\sqrt{n} g_{1,a} t\right) |SES\rangle_{a_1 a_2 \cdots a_n} |e\rangle_q \\ - \mathrm{i} \sin\left(\sqrt{n} g_{1,a} t\right) \prod_{j=1}^{n} |0\rangle_{a_j} |f\rangle_q. \end{aligned} \tag{4}$$

When the interaction time equals to $t_1 = \pi / \left(2\sqrt{n} g_{1,a}\right)$, the state transformation (4) becomes

$$|SES\rangle_{a_1 a_2 \cdots a_n} |e\rangle_q \to -\mathrm{i} \prod_{j=1}^{n} |0\rangle_{a_j} |f\rangle_q. \tag{5}$$

Based on Eq. (5), the initial state (2) of the whole system becomes

$$\left(\alpha |SES\rangle_{a_1 a_2 \cdots a_n} |g\rangle_q - \mathrm{i}\beta \prod_{j=1}^{n} |0\rangle_{a_j} |f\rangle_q\right) \prod_{j=1}^{n} |0\rangle_{b_j} \prod_{j=1}^{n} |0\rangle_{c_j}. \tag{6}$$

Step 2: Adjust the level spacings of the qutrit to have its $|g\rangle \leftrightarrow |e\rangle$ transition resonant with the n cavities $(a_1, a_2, \cdots, a_n)$ [Fig. 2(c)]. In the interaction picture and after the RWA, the Hamiltonian is given by

$$H_2 = g_{2,a} \sum_{j=1}^{n} \hat{a}_j |e\rangle_q \langle g| + \text{h.c.}, \tag{7}$$

where $g_{2,a}$ is the coupling constant between each of the cavities $(a_1, a_2, \cdots, a_n)$ and the $|g\rangle \leftrightarrow |e\rangle$ transition of the qutrit. Under the Hamiltonian (7), one has the following state transformation

$$\begin{aligned} |SES\rangle_{a_1 a_2 \cdots a_n} |g\rangle_q \to \cos\left(\sqrt{n} g_{2,a} t\right) |SES\rangle_{a_1 a_2 \cdots a_n} |g\rangle_q \\ - \mathrm{i} \sin\left(\sqrt{n} g_{2,a} t\right) \prod_{j=1}^{n} |0\rangle_{a_j} |e\rangle_q. \end{aligned} \tag{8}$$

When the interaction time equals to $t_2 = \pi / \left(2\sqrt{n} g_{2,a}\right)$, the state transformation (8) becomes

$$|SES\rangle_{a_1 a_2 \cdots a_n} |g\rangle_q \to -\mathrm{i} \prod_{j=1}^{n} |0\rangle_{a_j} |e\rangle_q. \tag{9}$$

Based on Eq. (9), the state (6) of the whole system becomes

$$\prod_{j=1}^{n} |0\rangle_{a_j} \left(\alpha |e\rangle_q + \beta |f\rangle_q\right) \prod_{j=1}^{n} |0\rangle_{b_j} \prod_{j=1}^{n} |0\rangle_{c_j}, \tag{10}$$

where a common phase factor "$-i$" has dropped off.

Step 3: Adjust the level spacings of the qutrit to have its $|g\rangle \leftrightarrow |e\rangle$ transition resonant with the n cavities $(b_1, b_2, \cdots, b_n)$ [Fig. 2(d)]. In the interaction picture and under the RWA, the Hamiltonian is given by

$$H_3 = g_b \sum_{j=1}^{n} \hat{b}_j |e\rangle_{q_1}\langle g| + \text{h.c.}, \tag{11}$$

where g_b is the coupling constant between the $|g\rangle \leftrightarrow |e\rangle$ transition of the qutrit and each of the n cavities $(b_1, b_2, \cdots, b_n)$.

When the qutrit interacts with the cavities $(b_1, b_2, \cdots, b_n)$ for a time t, one has the following state transformation under the Hamiltonian (11)

$$|e\rangle_q \prod_{j=1}^{n} |0\rangle_{b_j} \to \cos\left(\sqrt{n} g_b t\right) |e\rangle_q \prod_{j=1}^{n} |0\rangle_{b_j} - \mathrm{i} \sin\left(\sqrt{n} g_b t\right) |g\rangle_q |SES\rangle_{b_1 b_2 \cdots b_n}, \tag{12}$$

where $|SES\rangle_{b_1 b_2 \cdots b_n}$ is the SES entangled state of the cavities $(b_1, b_2, \cdots, b_n)$, which takes the same form as Eq. (1) with the subscripts $a_1 a_2 \cdots a_n$ replaced by $b_1 b_2 \cdots b_n$.

From Eq. (12), it can be seen that when $t_3 = \pi/\left(2\sqrt{n} g_b\right)$, one has

$$|e\rangle_q \prod_{j=1}^{n} |0\rangle_{b_j} \to -\mathrm{i} |g\rangle_q |SES\rangle_{b_1 b_2 \cdots b_n}. \tag{13}$$

Based on Eq. (13), the state (10) becomes

$$\prod_{j=1}^{n} |0\rangle_{a_j} \left(-\mathrm{i}\alpha |g\rangle_q |SES\rangle_{b_1 b_2 \cdots b_n} + \beta |f\rangle_q \prod_{j=1}^{n} |0\rangle_{b_j} \right) \prod_{j=1}^{n} |0\rangle_{c_j}. \tag{14}$$

Step 4: Adjust the level spacings of the qutrit to have its $|e\rangle \leftrightarrow |f\rangle$ transition resonant with the n cavities $(c_1, c_2, \cdots, c_n)$ [Fig. 2(e)]. In the interaction picture and under the RWA, the Hamiltonian is given by

$$H_4 = g_c \sum_{j=1}^{n} \hat{c}_j |f\rangle_q \langle e| + \text{h.c.}, \tag{15}$$

where g_c is the coupling constant between the $|e\rangle \leftrightarrow |f\rangle$ transition of the qutrit and each of the n cavities $(c_1, c_2, \cdots, c_n)$.

When the qutrit interacts with the cavities $(c_1, c_2, \cdots, c_n)$ for a time t, one has the following state transformation under the Hamiltonian (15)

$$|f\rangle_q \prod_{j=1}^{n} |0\rangle_{c_j} \to \cos\left(\sqrt{n} g_c t\right) |f\rangle_q \prod_{j=1}^{n} |0\rangle_{c_j} - \mathrm{i} \sin\left(\sqrt{n} g_c t\right) |e\rangle_q |SES\rangle_{c_1 c_2 \cdots c_n}, \tag{16}$$

where $|SES\rangle_{c_1 c_2 \cdots c_n}$ is the SES entangled state of the cavities $(c_1, c_2, \cdots, c_n)$, which takes the same form as Eq. (1) with the subscripts $a_1 a_2 \cdots a_n$ replaced by $c_1 c_2 \cdots c_n$.

From Eq. (16), it can be seen that when $t_4 = \pi/\left(2\sqrt{n} g_c\right)$, one has

$$|f\rangle_q \prod_{j=1}^{n} |0\rangle_{c_j} \to -\mathrm{i} |e\rangle_q |SES\rangle_{c_1 c_2 \cdots c_n}. \tag{17}$$

Based on Eq. (17), the state (14) becomes

$$\prod_{j=1}^{n} |0\rangle_{a_j} \left(\alpha |g\rangle_q |SES\rangle_{b_1 b_2 \cdots b_n} \prod_{j=1}^{n} |0\rangle_{c_j} + \beta |e\rangle_q \prod_{j=1}^{n} |0\rangle_{b_j} |SES\rangle_{c_1 c_2 \cdots c_n} \right), \tag{18}$$

where a common phase factor "$-i$" has dropped off. After this step of operation, one needs to adjust the level spacings of the qutrit back to its original configuration [Fig. 2(a)], such that the qutrit is decoupled from the cavity system.

Suppose that the two logic states of a photonic qubit are represented by the vacuum state $|0\rangle$ and the single photon state $|1\rangle$ of a cavity. Comparing Eq. (2) with Eq. (18), one can see that the SES entangled state (1) of n photonic qubits initially stored in the n cavities $(a_1, a_2, \cdots, a_n)$ at the input port is transferred onto: (i) the n cavities $(b_1, b_2, \cdots, b_n)$ at the output port 1 when the qutrit (the switch) is in the state $|g\rangle$, (ii) the n cavities $(c_1, c_2, \cdots, c_n)$ at the output port 2 when the qutrit (the switch) is in the state $|e\rangle$. This indicates that when the switch (the qutrit) is initially in a different state, the SES entangled state (1) of n photonic qubits is deterministically transferred from the n cavities at the input port to the n cavities at a different output port.

From the above description, one can find that:

(i) The total operational time for the entire state transfer is

$$\begin{aligned} t_{\text{op}} &= t_1 + t_2 + t_3 + t_4 + 2\tau_d \\ &= \pi/\left(2\sqrt{n} g_{1,a}\right) + \pi/\left(2\sqrt{n} g_{2,a}\right) + \pi/\left(2\sqrt{n} g_b\right) \\ &\quad + \pi/\left(2\sqrt{n} g_c\right) + 2\tau_d, \end{aligned} \tag{19}$$

where τ_d is the typical time required for adjusting the level spacings of the qutrit. From Eq. (19), one can see that the total operational time for the state transfer *decreases* as the number n of cavities (at the input port or each output port) increases.

(ii) Only qutrit-cavity resonant interactions are utilized. Hence, the state transfer can be fast performed and thus decoherence from the system is greatly suppressed.

(iii) The coupling or decoupling of the qutrit with the cavities is realized by adjusting the level spacings of the qutrit. For a superconducting device, its level spacings can be rapidly (within 1–3 ns) adjusted by varying external control parameters (e.g., magnetic flux applied to the superconducting loop of a SC phase, transmon, Xmon, or flux qubit or qutrit) [79–81]. Alternatively, the coupling or decoupling of the qutrit with the cavities can be obtained by adjusting the frequency of the cavities.

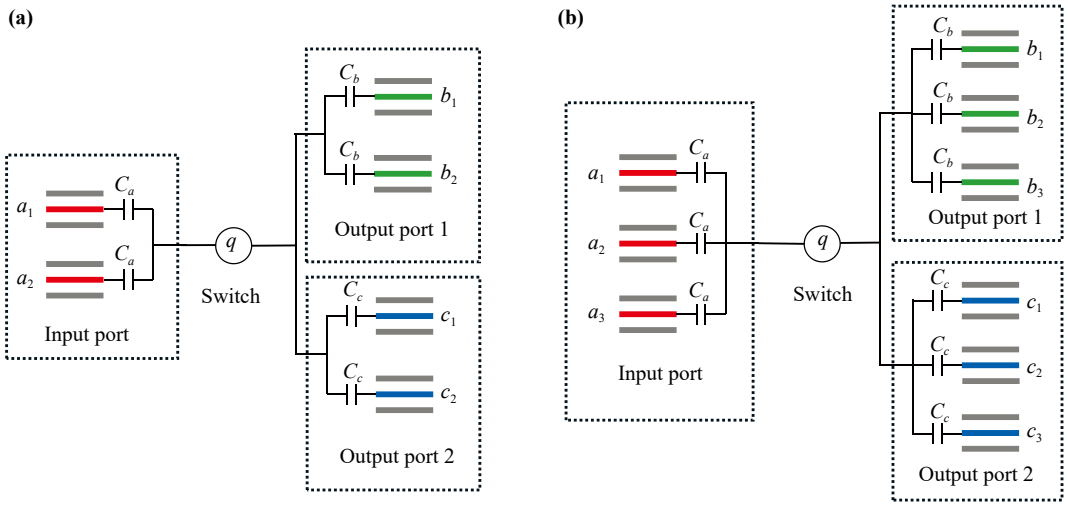

Fig. 3 Schematic diagram of the circuit-QED systems. **(a)** The system for the Bell state transfer. It consists of two cavities (a_1, a_2) at the input port, two cavities (b_1, b_2) at the output port 1, two cavities (c_1, c_2) at the output port 2, and a quantum switch composed of a transmon qutrit (q). **(b)** The system for the W state transfer. It consists of three cavities (a_1, a_2, a_3) at the input port, three cavities (b_1, b_2, b_3) at the output port 1, three cavities (c_1, c_2, c_3) at the output port 2, and a quantum switch composed of a transmon qutrit (q). In (a) and (b), each cavity is a 1D coplanar waveguide resonator, which is connected to the transmon qutrit via a capacitor.

For superconducting microwave cavities, their frequencies can be fast (within a few nanoseconds) tuned in experiments [82, 83].

In the above, we have considered a circuit-QED system, where the SC transmon qutrit (a three-level artificial atom) is coupled to the microwave cavities. The SES entangled state transfer is realized using the Hamiltonians (3), (7), (11) and (15). Notably, the three-level structure in Fig. 1(b) is available in an artificial atom with different types (e.g., a quantum dot, an NV center, a magnon, a SC qutrit of other types). By employing a three-level artificial atom to couple microwave or optical cavities, the same Hamiltonians (3), (7), (11) and (15) can in principle be obtained. Therefore, this proposal may be extended to realize the controlled transfer of the SES entangled state in other physical systems, where a three-level artificial atom couples to multiple microwave or optical cavities at the input port and the two output ports.

3 Experimental feasibility

As examples, we will investigate the experimental possibility of transferring the Bell state of two photonic qubits and the W state of three photonic qubits via a quantum switch. The setup for transferring the Bell state is shown in Fig. 3(a), which consists of two cavities (a_1, a_2) at the input port, two cavities (b_1, b_2) at the output port 1, two cavities (c_1, c_2) at the output port 2, and a quantum switch composed of a transmon qutrit q. Whereas, the setup for transferring the W state is shown in Fig. 3(b), which consists of three cavities (a_1, a_2, a_3) at the input port, three cavities (b_1, b_2, b_3) at the output port 1, three cavities (c_1, c_2, c_3) at the output port 2, and a quantum switch composed of a transmon qutrit q. In Figs. 3(a) and (b), each cavity is a one-dimensional (1D) coplanar waveguide cavity or resonator.

3.1 Ideal evolution states and initial states

The state transfer introduced in the previous Section 2 is realized in an ideal situation, i.e., the situation without considering the system dissipation, the unwanted couplings and the inter-cavity crosstalk. For the Bell state transfer, the ideal evolution state is the state given in Eq. (18) with $n = 2$, i.e.,

$$|\psi_{\mathrm{id}}\rangle = |00\rangle_{a_1a_2} \otimes \big(\alpha|g\rangle_q|Bell\rangle_{b_1b_2}|00\rangle_{c_1c_2} + \beta|e\rangle_q|00\rangle_{b_1b_2}|Bell\rangle_{c_1c_2}\big), \tag{20}$$

where $|Bell\rangle_{b_1b_2}$ $(|Bell\rangle_{c_1c_2})$ is the Bell state of two cavities (b_1, b_2) $[(c_1, c_2)]$, i.e., the SES entangled state given in Eq. (1) for $n = 2$, which is given by

$$|Bell\rangle_{b_1b_2} = \frac{1}{\sqrt{2}}\left(|01\rangle_{b_1b_2} + |10\rangle_{b_1b_2}\right),$$
$$|Bell\rangle_{c_1c_2} = \frac{1}{\sqrt{2}}\left(|01\rangle_{c_1c_2} + |10\rangle_{c_1c_2}\right). \tag{21}$$

According to Eq. (2), the initial state of the whole system for the Bell state transfer is

$$|\psi(0)\rangle = |Bell\rangle_{a_1a_2} \otimes (\alpha|g\rangle_q + \beta|e\rangle_q) \otimes |00\rangle_{b_1b_2}|00\rangle_{c_1c_2}, \tag{22}$$

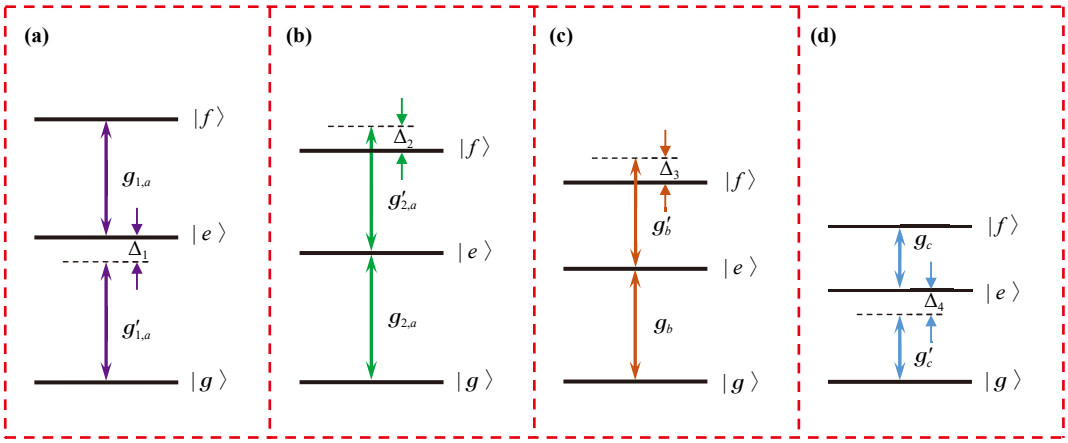

Fig. 4 Illustration of the cavities coupled to the transmon qutrit with the unwanted couplings considered. In **(a)**, the unwanted coupling between the cavities $(a_1, a_2, \cdots, a_n)$ and the $|g\rangle \leftrightarrow |e\rangle$ transition of the qutrit with coupling constant $g'_{1,a}$. In **(b)**, the unwanted coupling between the cavities $(a_1, a_2, \cdots, a_n)$ and the $|e\rangle \leftrightarrow |f\rangle$ transition of the qutrit with coupling constant $g'_{2,a}$. In **(c)**, the unwanted coupling of the cavities $(b_1, b_2, \cdots, b_n)$ with the $|e\rangle \leftrightarrow |f\rangle$ transition of the qutrit with coupling constant g'_b,. In **(d)**, the unwanted coupling of the cavities $(c_1, c_2, \cdots, c_n)$ with the $|g\rangle \leftrightarrow |e\rangle$ transition of the qutrit with coupling constant g'_c. Here, $n = 2$ for the Bell state transfer while $n = 3$ for the W state transfer. $\Delta_1, \Delta_2, \Delta_3$, and Δ_4 are detunings.

where the Bell state for the two input cavities (a_1, a_2) takes the same form as the Bell state given in Eq. (21).

On the other hand, for the W state transfer, the ideal output state is the state given in Eq. (18) with $n = 3$, i.e.,

$$|\psi_{\rm id}\rangle = |000\rangle_{a_1a_2a_3} \otimes \big(\alpha|g\rangle_q|W\rangle_{b_1b_2b_3}|000\rangle_{c_1c_2c_3} + \beta|e\rangle_q|000\rangle_{b_1b_2b_3}|W\rangle_{c_1c_2c_3}\big), \tag{23}$$

where $|W\rangle_{b_1b_2b_3}$ ($|W\rangle_{c_1c_2c_3}$) is the W state of three cavities (b_1, b_2, b_3) [(c_1, c_2, c_3)], i.e., the SES entangled state given in Eq. (1) for $n = 3$, which is given by

$$\begin{aligned} |W\rangle_{b_1b_2b_3} &= \frac{1}{\sqrt{3}}\left(|001\rangle_{b_1b_2b_3} + |010\rangle_{b_1b_2b_3} + |100\rangle_{b_1b_2b_3}\right), \\ |W\rangle_{c_1c_2c_3} &= \frac{1}{\sqrt{3}}\left(|001\rangle_{c_1c_2c_3} + |010\rangle_{c_1c_2c_3} + |100\rangle_{c_1c_2c_3}\right). \end{aligned} \tag{24}$$

According to Eq. (2), the initial state of the whole system for the W state transfer is

$$|\psi(0)\rangle = |W\rangle_{a_1a_2a_3} \otimes (\alpha|g\rangle_q + \beta|e\rangle_q) \otimes |000\rangle_{b_1b_2b_3}|000\rangle_{c_1c_2c_3}, \tag{25}$$

where the W state for the three input cavities (a_1, a_2, a_3) takes the same form as the W state given in Eq. (24).

3.2 Full Hamiltonians

As shown in the preceding Section 2, four basic Hamiltonians (3), (7), (11), and (15) are used for the state transfer. In reality, there exist the unwanted couplings between the qutrit and the cavities, as well as the inter-cavity crosstalks. We will give the modification on these Hamiltonians when they are taken into account. In the following, $n = 2$ for the Bell state transfer, while $n = 3$ for the W state transfer.

(i) The Hamiltonian (3) is modified as follows $\widetilde{H}_1 = H_1 + \delta H_1 + \varepsilon$, where δH_1 describes the unwanted coupling between the $|g\rangle \leftrightarrow |e\rangle$ transition of the qutrit and the cavities $(a_1, a_2, \cdots, a_n)$ [Fig. 4(a)], while ε describes the inter-cavity crosstalks. The expression of δH_1 is given by

$$\delta H_1 = g'_{1,a} e^{i\Delta_1 t} \sum_{j=1}^{n} \hat{a}_j |e\rangle_q\langle g| + \text{h.c.}, \tag{26}$$

where $g'_{1,a}$ is the off-resonant coupling constant between the $|g\rangle \leftrightarrow |e\rangle$ transition of the qutrit and the cavities $(a_1, a_2, \cdots, a_n)$, and $\Delta_1 = \omega_{fe} - \omega_a > 0$ is the detuning between the $|g\rangle \leftrightarrow |e\rangle$ transition frequency ω_{fe} of the qutrit and the frequency ω_a of the cavities $(a_1, a_2, \cdots, a_n)$. Here and below, the expression of ε is given by

$$\begin{aligned} \varepsilon = {} & g_{aa} \sum_{j,k=1;j\neq k}^{n} \hat{a}_j\hat{a}_k^+ + g_{bb} \sum_{j,k=1;j\neq k}^{n} \hat{b}_j\hat{b}_k^+ \\ & + g_{cc} \sum_{j,k=1;j\neq k}^{n} \hat{c}_j\hat{c}_k^+ + g_{ab} e^{-i\Delta_{ab}t} \sum_{j,k=1;j\neq k}^{n} \hat{a}_j\hat{b}_k^+ \\ & + g_{ac} e^{-i\Delta_{ac}t} \sum_{j,k=1;j\neq k}^{n} \hat{a}_j\hat{c}_k^+ \\ & + g_{bc} e^{-i\Delta_{bc}t} \sum_{j,k=1;j\neq k}^{n} \hat{b}_j\hat{c}_k^+ + \text{h.c.}, \end{aligned} \tag{27}$$

where the first term describes the inter-cavity crosstalk between the cavities $(a_1, a_2, \cdots, a_n)$ with crosstalk strength g_{aa}, the second term describes the inter-cavity crosstalk between the cavities $(b_1, b_2, \cdots, b_n)$ with crosstalk strength g_{bb}, the third term describes the inter-cavity crosstalk between the cavities $(c_1, c_2, \cdots, c_n)$ with crosstalk strength g_{cc}, the fourth term describes the inter-cavity crosstalk between the cavities $(a_1, a_2, \cdots, a_n)$ and the cavities $(b_1, b_2, \cdots, b_n)$ with crosstalk strength g_{ab} and frequency detuning $\Delta_{ab} = \omega_a - \omega_b$, the fifth term describes the inter-cavity crosstalk between the cavities $(a_1, a_2, \cdots, a_n)$ and the cavities $(c_1, c_2, \cdots, c_n)$ with crosstalk strength g_{ac} and frequency detuning $\Delta_{ac} = \omega_a - \omega_c$, and the sixth term describes the inter-cavity crosstalk between the cavities $(b_1, b_2, \cdots, b_n)$ and the cavities $(c_1, c_2, \cdots, c_n)$ with crosstalk strength g_{bc} and frequency detuning $\Delta_{bc} = \omega_b - \omega_c$. The inter-cavity crosstalk between any two of the three sets of cavities $(a_1, a_2, \cdots, a_n)$, cavities $(b_1, b_2, \cdots, b_n)$, and cavities $(c_1, c_2, \cdots, c_n)$ can be reduced by increasing the ratio of Δ_{ab}/g_{ab}, Δ_{ac}/g_{ac}, and Δ_{bc}/g_{bc}. The primary causes of inter-cavity crosstalk stem from two mechanisms: imperfect capacitive coupling between the transmom and the cavities, and energy leakage from the open structure of the waveguide cavities, leading to unintended energy transfer between the cavities.

(ii) The Hamiltonian (7) is modified as follows $\widetilde{H}_2 = H_2 + \delta H_2 + \varepsilon$, where δH_2 describes the unwanted coupling between the $|e\rangle \leftrightarrow |f\rangle$ transition of the qutrit and the cavities $(a_1, a_2, \cdots, a_n)$ [Fig. 4(b)]. The expression of δH_2 is given by

$$\delta H_2 = g'_{2,a} \mathrm{e}^{\mathrm{i}\Delta_2 t} \sum_{j=1}^{n} \hat{a}_j |f\rangle_q \langle e| + \mathrm{h.c.}, \tag{28}$$

where $g'_{2,a}$ is the off-resonant coupling constant between the $|e\rangle \leftrightarrow |f\rangle$ transition of the qutrit and the cavities $(a_1, a_2, \cdots, a_n)$, and $\Delta_2 = \omega_{fe} - \omega_a < 0$ is the detuning between the $|e\rangle \leftrightarrow |f\rangle$ transition frequency ω_{fe} of the qutrit and the frequency ω_a of the cavities $(a_1, a_2, \cdots, a_n)$.

(iii) The Hamiltonian (11) is modified as follows: $\widetilde{H}_3 = H_3 + \delta H_3 + \varepsilon$, where δH_3 describes the unwanted interaction between the $|e\rangle \leftrightarrow |f\rangle$ transition of the qutrit and the cavities $(b_1, b_2, \cdots, b_n)$ [Fig. 4(c)]. The expression of δH_3 is given by

$$\delta H_3 = g'_b \mathrm{e}^{\mathrm{i}\Delta_3 t} \sum_{j=1}^{n} \hat{b}_j |f\rangle_q \langle e| + \mathrm{h.c.}, \tag{29}$$

where g'_b is the off-resonant coupling constant between the $|e\rangle \leftrightarrow |f\rangle$ transition of the qutrit and the cavities $(b_1, b_2, \cdots, b_n)$, and $\Delta_3 = \omega_{fe} - \omega_b < 0$ is the detuning between the $|e\rangle \leftrightarrow |f\rangle$ transition frequency ω_{fe} of the qutrit and the frequency ω_b of the cavities $(b_1, b_2, \cdots, b_n)$.

(iv) The Hamiltonian (15) is modified as follows $\widetilde{H}_4 = H_4 + \delta H_4 + \varepsilon$, where δH_4 describes the unwanted interaction between the qutrit and the cavities $(c_1, c_2, \cdots, c_n)$ [Fig. 4(d)]. The expression of δH_4 is given by

$$\delta H_4 = g'_c \mathrm{e}^{\mathrm{i}\Delta_4 t} \sum_{j=1}^{n} \hat{c}_j |e\rangle_q \langle g| + \mathrm{h.c.}, \tag{30}$$

where g'_c is the off-resonant coupling constant between the $|g\rangle \leftrightarrow |e\rangle$ transition of the qutrit and the cavities $(c_1, c_2, \cdots, c_n)$, and $\Delta_4 = \omega_{eg} - \omega_c > 0$ is the detuning between the $|g\rangle \leftrightarrow |e\rangle$ transition frequency ω_{eg} of the qutrit and the frequency ω_c of $(c_1, c_2, \cdots, c_n)$.

For a transmon qutrit, the $|g\rangle \leftrightarrow |f\rangle$ transition is forbidden or very weak [84]. Accordingly, the coupling of the cavities with the $|g\rangle \leftrightarrow |f\rangle$ transition of the qutrit can be neglected and thus is not considered in the above modified Hamiltonians.

3.3 Numerical results

When considering the relaxation and dephasing of the qutrit as well as the cavity decay, the dynamics of the lossy system is determined by the following master equation

$$\begin{aligned} \frac{\mathrm{d}\rho}{\mathrm{d}t} = & -\mathrm{i}\left[\widetilde{H}_k, \rho\right] + \sum_{j=1}^{n} \left(\kappa_{a_j} \mathcal{L}\left[\hat{a}_j\right] + \kappa_{b_j} \mathcal{L}\left[\hat{b}_j\right] \right. \\ & \left. + \kappa_{c_j} \mathcal{L}\left[\hat{c}_j\right] \right) + \gamma_{eg} \mathcal{L}\left[\sigma_{eg}^{-}\right] + \gamma_{fe} \mathcal{L}\left[\sigma_{fe}^{-}\right] \\ & + \gamma_{fg} \mathcal{L}\left[\sigma_{fg}^{-}\right] + \gamma_{e,\varphi} \mathcal{L}\left[\sigma_{ee}\right] + \gamma_{f,\varphi} \mathcal{L}\left[\sigma_{ff}\right], \end{aligned} \tag{31}$$

where ρ is the density operator of the whole system at time t, $\widetilde{H}_k$ $(k = 1, 2, 3, 4)$ is the modified Hamiltonian given above, $\sigma_{eg}^{-} = |g\rangle_q\langle e|, \sigma_{fe}^{-} = |e\rangle_q\langle f|, \sigma_{fg}^{-} = |g\rangle_q\langle f|$, $\sigma_{ee} = |e\rangle_q\langle e|, \sigma_{ff} = |f\rangle_q\langle f|$, $\mathcal{L}[\Lambda] = \Lambda\rho\Lambda^{+} - \Lambda^{+}\Lambda\rho/2 - \rho\Lambda^{+}\Lambda/2$ (with $\Lambda = \hat{a}_j, \hat{b}_j, \hat{c}_j, \sigma_{eg}^{-}, \sigma_{fe}^{-}, \sigma_{fg}^{-}, \sigma_{ee}, \sigma_{ff}$); $\kappa_{a_j}, \kappa_{b_j}$, and κ_{c_j} are the decay rates of cavity a_j, cavity b_j, and cavity c_j, respectively; γ_{eg} is the energy relaxation rate of the level $|e\rangle$, γ_{fe} (γ_{fg}) is the relaxation rate of the level $|f\rangle$ for the decay path $|f\rangle \to |e\rangle$ $(|f\rangle \to |g\rangle)$ of the qutrit; $\gamma_{e,\varphi}$ $(\gamma_{f,\varphi})$ is the dephasing rate of the level $|e\rangle$ $(|f\rangle)$ of the qutrit.

Without loss of generality, we consider arbitrary numbers α and β, by setting $\alpha = \cos(\theta/2)$ and $\beta = \mathrm{e}^{\mathrm{i}\varphi}\sin(\theta/2)$. The average fidelity of the operation is defined by [85]

$$\overline{\mathcal{F}} = \frac{1}{4\pi} \int_0^{2\pi} \mathrm{d}\varphi \int_0^{\pi} \mathcal{F} \sin\theta \mathrm{d}\theta, \tag{32}$$

with

$$\mathcal{F} = \sqrt{\langle \psi_{\mathrm{id}} | \rho_f | \psi_{\mathrm{id}} \rangle}, \tag{33}$$

where $|\psi_{\mathrm{id}}\rangle$ is the ideal evolution state given in Eq. (20) for the Bell state transfer while the ideal evolution state given in Eq. (23) for the W state transfer; ρ_f is the final

Table 1 Parameters used in the numerical simulations. For the definitions of the parameters, please refer to the text.

Transition frequencies of qutrits (q) for level structure (step 1)	$\omega_{eg}/(2\pi) = 6.2$ GHz	$\omega_{fe}/(2\pi) = 5.8$ GHz	$\omega_{fg}/(2\pi) = 12.0$ GHz
Transition frequencies of qutrits (q) for level structure (step 2)	$\omega_{eg}/(2\pi) = 5.8$ GHz	$\omega_{fe}/(2\pi) = 5.4$ GHz	$\omega_{fg}/(2\pi) = 11.2$ GHz
Transition frequencies of qutrits (q) for level structure (step 3)	$\omega_{eg}/(2\pi) = 5.4$ GHz	$\omega_{fe}/(2\pi) = 5.0$ GHz	$\omega_{fg}/(2\pi) = 10.4$ GHz
Transition frequencies of qutrits (q) for level structure (step 4)	$\omega_{eg}/(2\pi) = 5.0$ GHz	$\omega_{fe}/(2\pi) = 4.6$ GHz	$\omega_{fg}/(2\pi) = 9.6$ GHz
Cavity frequencies	$\omega_a/(2\pi) = 5.8$ GHz	$\omega_b/(2\pi) = 5.4$ GHz	$\omega_c/(2\pi) = 4.6$ GHz
Detunings	$\Delta_1/(2\pi) = 0.4$ GHz	$\Delta_2/(2\pi) = -0.4$ GHz	$\Delta_3/(2\pi) = -0.4$ GHz
	$\Delta_4/(2\pi) = 0.4$ GHz	$\Delta_{ab}/(2\pi) = 0.4$ GHz	$\Delta_{ac}/(2\pi) = 1.2$ GHz
	$\Delta_{bc}/(2\pi) = 0.8$ GHz		
Coupling constants	$g_{1,a}/(2\pi) = 10$ MHz	$g'_{1,a}/(2\pi) = 7.07$ MHz	$g_{2,a}/(2\pi) = 7.07$ MHz
	$g'_{2,a}/(2\pi) = 10$ MHz	$g_b/(2\pi) = 7.07$ MHz	$g'_b/(2\pi) = 10$ MHz
	$g_c/(2\pi) = 10$ MHz	$g'_c/(2\pi) = 7.07$ MHz	

density operator of the system when the operation is performed in a realistic situation, i.e., the situation which considers the system dissipation, the unwanted couplings, and the inter-cavity crosstalk. The density operator ρ_f is obtained by numerically solving the master equation (31) with the initial state given in Eq. (22) for the Bell state transfer and the initial state given in Eq. (25) for the W state transfer.

Experimentally, the frequency of a microwave cavity can be made as 2−51 GHz [22, 86], the typical transition frequency between neighboring levels of a transmon qutrit can be made to be 2−20 GHz [86, 87], and the level spacing anharmonicity 100−720 MHz of a transmon qutrit has been reported [88]. For a transmon qutrit [84], $g'_{1,a} = g_{1,a}/\sqrt{2}$, $g'_{2,a} = \sqrt{2}g_{2,a}, g'_b = \sqrt{2}g_b$, and $g'_c = g_c/\sqrt{2}$. As a concrete example, let us consider the parameters listed in Table 1, which are used in our numerical simulations. Other parameters used in the numerical simulations are: (i) $\gamma_{eg}^{-1} = 60$ μs, $\gamma_{fe}^{-1} = 30$ μs, $\gamma_{fg}^{-1} = 150$ μs [89], (ii) $\gamma_{f,\varphi}^{-1} = \gamma_{e,\varphi}^{-1} = 20$ μs, (iii) $\kappa_{a_j}^{-1} = \kappa_{b_j}^{-1} = \kappa_{c_j}^{-1} \equiv \kappa^{-1}$, and (iv) $g_{aa} = g_{bb} = g_{cc} = g_{ab} = g_{ac} = g_{bc} \equiv g_{cr}$. The decoherence times of the transmon qutrits considered here are a rather conservative case because energy relaxation time with a range from 65 μs to 0.5 ms and dephasing time from 25 to 75 μs have been experimentally demonstrated for a superconducting transmon device [12–14, 90, 91]. For the coupling constants listed in Table 1, one has $g_{\max} = \max\{g_{1,a}, g'_{1,a}, g_{2,a}, g'_{2,a}, g_b, g'_b, g_c, g'_c\} = 2\pi \times 10$ MHz. Note that coupling strengths of ~ 10 MHz between SC transmons and cavities have been reported in Refs. [92–94], and a coupling strength $2\pi \times 897$ MHz has been reported for a transmon coupled to a 1D transmission line resonator [95]. In addition, the Rabi frequency $2\pi \times 300$ MHz of a classical microwave pulse was reported in experiments [96].

By numerically solving the master equation (31), we plot Fig. 5 showing the average fidelity versus $g_{cr}/g_{\max}$ and κ^{-1} for the Bell state transfer and Fig. 6 showing the average fidelity versus $g_{cr}/g_{\max}$ and κ^{-1} for the W state transfer. Figures 5 and 6 show that the influence of the inter-cavity crosstalk is very small for a given κ^{-1}. In addition, even when $g_{cr} = 0.1 g_{\max}$, for $\kappa^{-1} = 20$ μs, a high average fidelity 99.56% can be obtained for the Bell state transfer and a high average fidelity 99.25% can be achieved for the W state transfer.

To examine how the cavity number n of the transferred entangled state influences the result, Fig. 7 displays the average fidelity versus the qutrit decoherence time T for $n = 2$, 3, 4 and 5. The relaxation rates are set to $\gamma_{eg}^{-1} = 3T$, $\gamma_{fe}^{-1} = 1.5T$, $\gamma_{fg}^{-1} = 7.5T$ and the dephasing rates to $\gamma_{f,\varphi}^{-1} = \gamma_{e,\varphi}^{-1} = T$, while $\kappa^{-1} = 20$ μs and $g_{cr}/g_{\max} = 0.01$. As expected, the fidelity depends weakly on T, since the entire protocol involves only one qutrit. The fidelity decreases slowly as n increases. The reason for this is as follows. Because only resonant interactions are employed, the total operational time is extremely short

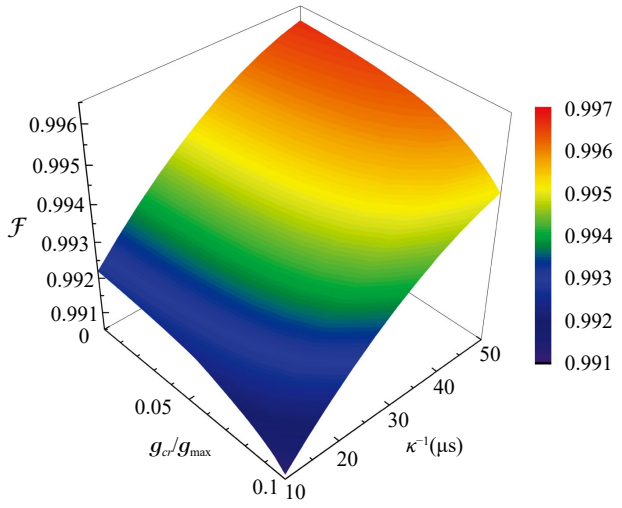

Fig. 5 Fidelity $\mathcal{F}$ versus κ^{-1} and $g_{cr}/g_{\max}$ for the Bell state transfer.

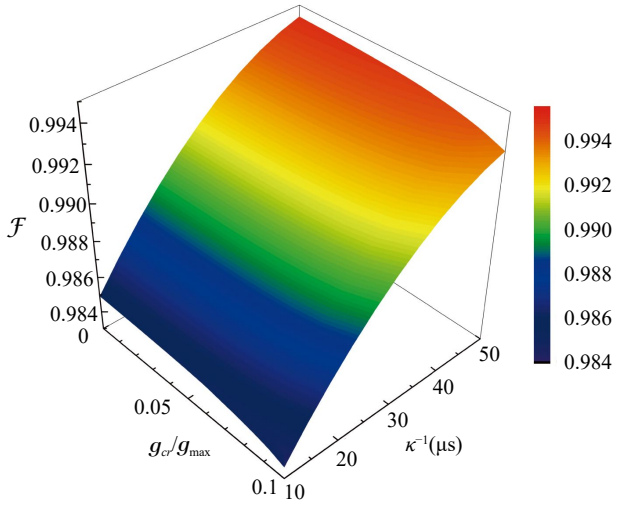

Fig. 6 Fidelity $\mathcal{F}$ versus κ^{-1} and $g_{cr}/g_{\max}$ for the W state transfer.

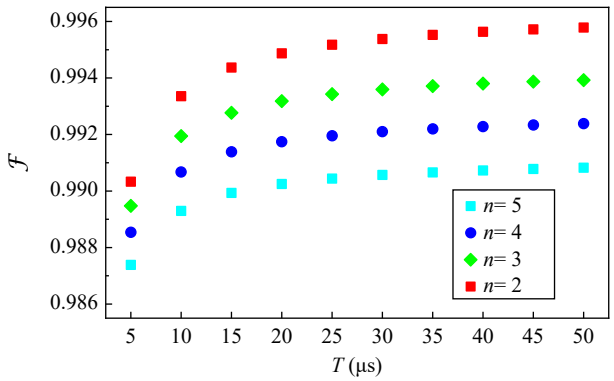

Fig. 7 Fidelity $\mathcal{F}$ versus the qutrit decoherence time T for $n = 2, 3, 4,$ and 5.

and, according to Eq. (19), actually becomes shorter for a larger n.

With the parameters chosen above, the operational time is estimated as 74 ns for the Bell state transfer and 69 ns for the W state transfer (assuming $\tau_d = 2$ ns), which is much shorter than the decoherence times of the qutrits and the cavity decay times (10−50 μs), used in the numerical simulation. For the cavity frequencies given above and $\kappa^{-1} = 20$ μs, the quality factors of the cavities at the input port, the output port 1 and the output port 2 are, respectively, $Q_a \sim 4.52 \times 10^5$, $Q_b \sim 3.96 \times 10^5$, and $Q_c \sim 3.39 \times 10^5$, which are available because a 1D microwave cavity or resonator with a high quality factor $Q \gtrsim 2.7 \times 10^6$ was experimentally reported [97, 98]. The analysis given above demonstrates that the high-fidelity controlled transfer of the Bell state and the W state is feasible with the present circuit QED technology.

3.4 Discussion

As seen in Table 1, the ratio of detuning values by the unwanted qutrit-cavity coupling constants falls within 35 to 47, which means that the cavities are highly detuned from the transitions between the irrelevant levels of the qutrit. In this sense, the effect of the unwanted qutrit-cavity couplings on the fidelity is negligibly small.

In our numerical calculations, we adopt a conservative scenario where $g_{cr} \leq 0.1 g_{\max}$, which is significantly more stringent than the typical scenario in circuit QED, where the inter-cavity crosstalk g_{cr} is usually two to three orders of magnitude weaker than the maximum coupling strength $g_{\max}$ [71, 99, 100]. In addition, from Table 1, one can see that the frequency detunings between any two of the cavity frequencies ω_a, ω_b, and ω_c are greater than the inter-cavity crosstalk strength g_{cr} by at least two orders of magnitude (even for $g_{cr} = 0.1 g_{\max}$). Therefore, the influence of the inter-cavity crosstalk between the input port and either of the two output ports or between the two output ports can be neglected. Notably, one can verify that the SES entangled states of the cavities at the input port, the output port 1 and the output port 2 are, respectively, the eigenstates of the first three terms in Eq. (27). This indicates that, in principle, the inter-cavity crosstalk within the input port or either of the two output ports has no influence on the SES entangled state transfer.

The infidelity mainly results from the qutrit decoherence, the cavity dissipation, and the unwanted qutrit-cavity interaction. The fidelity can be improved by: designing the qutrit with larger level spacing anharmonicity, choosing the qutrit with longer decoherence time, and selecting the cavities with a high quality factor.

We have assumed that a pure initial state (i.e., SES entangled state) at the input port can be prepared. Suppressing the thermal photon background is crucial for ensuring the purity of the initial state in experiments. To address this challenge, quantum devices are typically placed within a dilution refrigerator, where the base temperature can be stably maintained at an ultra-low level of approximately 10 mK [101]. Furthermore, techniques, such as the Derivative Removal for Annulment of Cavity-Hybridized Measurement Adiabat (DRACHMA), can be employed to reduce the thermal photon occupancy to on the order of 10^{-3} within a short time frame [101, 102].

For simplicity, our numerical simulation did not consider: (i) The coupling of the cavities with the $|g\rangle \leftrightarrow |f\rangle$ transition, and (ii) The qutrit decoherence and the cavity dissipation during the adjustment of the qutrit level spacings. However, we remark that when they are taken into account, the fidelity would be slightly decreased. This is because: (i) The coupling of the cavities with the $|g\rangle \leftrightarrow |f\rangle$ transition is negligible

because of the very weak $|g\rangle \leftrightarrow |f\rangle$ transition for the transmon qutrit, (ii) The effect of the qutrit decoherence and the cavity dissipation, during the adjustment of the qutrit level spacings, is negligible because the level spacings of a superconducting qutrit can be rapidly adjusted within 1−3 ns [79–81]. We remark that further investigation is needed for each particular experimental setup. However, this requires a rather lengthy and complex analysis, which is beyond the scope of this theoretical work.

4 Conclusions

We have proposed to transfer the single-excitation symmetric (SES) entangled state of n photonic qubits from n microwave cavities at the input port to the n microwave cavities at either of the two output ports via the control of a quantum switch. This proposal has the features and advantages described in the introduction. Since the SES entangled state is a W-type entangled state for $n \geq 3$ and a Bell entangled state for $n = 2$, the proposal can be used to transfer both W state and Bell state of photonic qubits via the control of a quantum switch. As an example, we have numerically analyzed the circuit-QED experimental feasibility of transferring both the Bell state of two photonic qubits and the W state of three photonic qubits in a control manner.

To verify the success of the state transfer, one can measure the SES entangled state at the output ports using the following architecture: in the system depicted in Fig. 1(a), each cavity at the output ports needs to be independently coupled to an ancillary SC qubit. By performing controlled gate operations between each cavity and each corresponding ancillary qubit, the SES entangled state of the cavities can be transferred to the ancillary qubits. Subsequently, by measuring the quantum state of each ancillary qubit — for instance, using techniques such as quantum state tomography — the SES entangled state in the cavities can be measured and determined.

To the best of our knowledge, this work is the first to show the transfer of quantum entangled states of photonic qubits from the microwave cavities at the input port to the microwave cavities at either of two output ports via a quantum switch. This proposal may be extended to accomplish the same task in other physical systems, where the quantum switch is implemented with an artificial atom (e.g., a quantum dot, an NV center, a magnon, and a SC qutrit with different types, etc.) and each cavity is a microwave or optical cavity. Our results provide new insights into controlled transfer of quantum entangled states. They may have potential applications in networked quantum communication, distributed quantum information processing, as well as development of quantum functional devices (e.g., quantum triodes and quantum routers). We hope that it could stimulate the experimental activities in the near future.

Declarations The authors declare that they have no competing interests and there are no conflicts.

Acknowledgements This work was partly supported by the National Key Research and Development Program of China (Grant No. 2024YFA1408900), the National Natural Science Foundation of China (NSFC) (Grant Nos. 11074062, 11374083, 11774076, 11974096, and U21A20436), and the Innovation Program for Quantum Science and Technology (No. 2021ZD0301705).

References and notes

1. J. Q. You and F. Nori, Atomic physics and quantum optics using superconducting circuits, *Nature* 474(7353), 589 (2011)
2. Y. Makhlin, G. Schon, and A. Shnirman, Quantum-state engineering with Josephson-junction devices, *Rev. Mod. Phys.* 73(2), 357 (2001)
3. M. Devoret, S. Girvin, and R. Schoelkopf, Circuit-QED: How strong can the coupling between a Josephson junction atom and a transmission line resonator be, *Ann. Phys.* 519(10–11), 767 (2007)
4. P. Krantz, M. Kjaergaard, F. Yan, T. P. Orlando, S. Gustavsson, and W. D. Oliver, A quantum engineer's guide to superconducting qubits, *Appl. Phys. Rev.* 6(2), 021318 (2019)
5. A. Blais, S. M. Girvin, and W. D. Oliver, Quantum information processing and quantum optics with circuit quantum electrodynamics, *Nat. Phys.* 16(3), 247 (2020)
6. Q. P. Su, Y. Zhang, L. Bin, and C. P. Yang, Efficient scheme for realizing a multiplex-controlled phase gate with photonic qubits in circuit quantum electrodynamics, *Front. Phys. (Beijing)* 17(5), 53505 (2022)
7. C. P. Yang, J. H. Ni, L. Bin, Y. Zhang, Y. Yu, and Q. P. Su, Preparation of maximally-entangled states with multiple cat-state qutrits in circuit QED, *Front. Phys. (Beijing)* 19(3), 31201 (2024)
8. X. L. Li, Z. Tao, K. Yi, K. Luo, L. Zhang, Y. Zhou, S. Liu, T. Yan, Y. Chen, and D. Yu, Hardware-efficient and fast three-qubit gate in superconducting quantum circuits, *Front. Phys. (Beijing)* 19(5), 51205 (2024)
9. A. Wallraff, D. I. Schuster, A. Blais, L. Frunzio, R. S. Huang, J. Majer, S. Kumar, S. M. Girvin, and R. J. Schoelkopf, Strong coupling of a single photon to a superconducting qubit using circuit quantum electrodynamics, *Nature* 431(7005), 162 (2004)
10. T. Niemczyk, F. Deppe, H. Huebl, E. P. Menzel, F. Hocke, M. J. Schwarz, J. J. Garcia-Ripoll, D. Zueco, T. Hümmer, E. Solano, A. Marx, and R. Gross, Circuit quantum electrodynamics in the ultrastrong-coupling regime, *Nat. Phys.* 6(10), 772 (2010)
11. P. Forn-Díaz, J. Lisenfeld, D. Marcos, J. J. García-Ripoll, E. Solano, C. J. P. M. Harmans, and J. E. Mooij, Observation of the Bloch-Siegert shift in a qubit-oscillator system in the ultrastrong coupling regime,

Phys. Rev. Lett. 105(23), 237001 (2010)
12. A. P. M. Place, L. V. H. Rodgers, P. Mundada, B. M. Smitham, M. Fitzpatrick, Z. Leng, A. Premkumar, J. Bryon, A. Vrajitoarea, S. Sussman, G. Cheng, T. Madhavan, H. K. Babla, X. H. Le, Y. Gang, B. Jäck, A. Gyenis, N. Yao, R. J. Cava, N. P. de Leon, and A. A. Houck, New material platform for superconducting transmon qubits with coherence times exceeding 0.3 milliseconds, *Nat. Commun.* 12(1), 1779 (2021)
13. S. Kono, J. Pan, M. Chegnizadeh, X. Wang, A. Youssefi, M. Scigliuzzo, and T. J. Kippenberg, Mechanicall induced correlated errors on superconducting qubits with relaxation times exceeding 0.4 milliseconds, *Nat. Commun.* 15, 3950 (2024)
14. C. Wang, X. Li, H. Xu, Z. Li, J. Wang, et al., Towards practical quantum computers transmon qubit with a lifetime approaching 0.5 milliseconds, *npj Quantum Inf.* 8, 3 (2022)
15. F. Yan, S. Gustavsson, A. Kamal, J. Birenbaum, A. P. Sears, D. Hover, T. J. Gudmundsen, D. Rosenberg, G. Samach, S. Weber, J. L. Yoder, T. P. Orlando, J. Clarke, A. J. Kerman, and W. D. Oliver, The flux qubit revisited to enhance coherence and reproducibility, *Nat. Commun.* 7(1), 12964 (2016)
16. A. Somoroff, Q. Ficheux, R. A. Mencia, H. N. Xiong, R. Kuzmin, and V. E. Manucharyan, Millisecond coherence in a superconducting qubit, *Phys. Rev. Lett.* 130(26), 267001 (2023)
17. M. Reagor, W. Pfaff, C. Axline, R. W. Heeres, N. Ofek, K. Sliwa, E. Holland, C. Wang, J. Blumoff, K. Chou, M. J. Hatridge, L. Frunzio, M. H. Devoret, L. Jiang, and R. J. Schoelkopf, A quantum memory with near-millisecond coherence in circuit QED, *Phys. Rev. B* 94(1), 014506 (2016)
18. M. Kudra, J. Biznarova, A. Fadavi Roudsari, J. J. Burnett, D. Niepce, S. Gasparinetti, B. Wickman, and P. Delsing, High quality three-dimensional aluminum microwave cavities, *Appl. Phys. Lett.* 117(7), 070601 (2020)
19. A. Romanenko, R. Pilipenko, S. Zorzetti, D. Frolov, M. Awida, S. Belomestnykh, S. Posen, and A. Grassellino, Three dimensional superconducting resonators at $T < 20$ mK with photon lifetimes up to $\tau = 2$ s, *Phys. Rev. Appl.* 13(3), 034032 (2020)
20. J. Q. You and F. Nori, Superconducting circuits and quantum information, *Phys. Today* 58(11), 42 (2005)
21. X. Gu, A. F. Kockum, A. Miranowicz, Y. X. Liu, and F. Nori, Microwave photonics with superconducting quantum circuits, *Phys. Rep.* 718–719, 1 (2017)
22. A. Blais, A. L. Grimsmo, S. M. Girvin, and A. Wallraff, Circuit quantum electrodynamics, *Rev. Mod. Phys.* 93(2), 025005 (2021)
23. G. Wendin, Quantum information processing with superconducting circuits: A review, *Rep. Prog. Phys.* 80(10), 106001 (2017)
24. C. P. Yang, S. I. Chu, and S. Han, Possible realization of entanglement, logical gates, and quantum-information transfer with superconducting-quantum-interference-device qubits in cavity QED, *Phys. Rev. A* 67(4), 042311 (2003)
25. C. P. Yang, S. I. Chu, and S. Han, Quantum information transfer and entanglement with SQUID qubits in cavity QED: A dark-state scheme with tolerance for nonuniform device parameter, *Phys. Rev. Lett.* 92(11), 117902 (2004)
26. Z. Kis and E. Paspalakis, Arbitrary rotation and entanglement of flux SQUID qubits, *Phys. Rev. B* 69(2), 024510 (2004)
27. E. Paspalakis and N. J. Kylstra, Coherent manipulation of superconducting quantum interference devices with adiabatic passage, *J. Mod. Opt.* 51(11), 1679 (2004)
28. C. P. Yang, Quantum information transfer with superconducting flux qubits coupled to a resonator, *Phys. Rev. A* 82(5), 054303 (2010)
29. C. P. Yang, Q. P. Su, and F. Nori, Entanglement generation and quantum information transfer between spatially-separated qubits in different cavities, *New J. Phys.* 15(11), 115003 (2013)
30. Y. He and Y. X. Zhang, Quantum state transfer via a multimode resonator, *Phys. Rev. Lett.* 134(2), 023602 (2025)
31. S. Salimian and M. K. Tavassoly, Quantum information transfer and entangled state generation using superconducting qubits in the absence and presence of dissipation, *Eur. Phys. J. Plus* 135(7), 594 (2020)
32. X. Q. Liu, J. Liu, and Z. Y. Xue, Robust and fast quantum state transfer on superconducting circuits, *JETP Lett.* 117(11), 859 (2023)
33. S. Singh, B. Adhikari, S. Dutta, and D. Zueco, Perfect state transfer on hypercubes and its implementation using superconducting qubits, *Phys. Rev. A* 102(6), 062609 (2020)
34. M. Malekakhlagh, T. Phung, D. Puzzuoli, K. Heya, N. Sundaresan, and J. Orcutt, Enhanced quantum state transfer and Bell-state generation over long-range multimode interconnects via superadiabatic transitionless driving, *Phys. Rev. Appl.* 22(2), 024006 (2024)
35. Y. X. Wu, Z. Y. Guan, S. Li, and Z. Y. Xue, Fast quantum state transfer and entanglement for cavity-coupled many qubits via dark pathways, *Front. Phys. (Beijing)* 17(4), 42507 (2022)
36. J. N. Zhang, J. X. Han, J. L. Wu, J. Song, and Y. Y. Jiang, Robust beam splitter with fast quantum state transfer through a topological interface, *Front. Phys. (Beijing)* 18(5), 51303 (2023)
37. M. A. Sillanpää, J. I. Park, and R. W. Simmonds, Coherent quantum state storage and transfer between two phase qubits via a resonant cavity, *Nature* 449(7161), 438 (2007)
38. J. Majer, J. M. Chow, J. M. Gambetta, J. Koch, B. R. Johnson, J. A. Schreier, L. Frunzio, D. I. Schuster, A. A. Houck, A. Wallraff, A. Blais, M. H. Devoret, S. M. Girvin, and R. J. Schoelkopf, Coupling superconducting qubits via a cavity bus, *Nature* 449(7161), 443 (2007)
39. D. Li, W. Zheng, J. Chu, X. Yang, S. Song, Z. Han, Y. Dong, Z. Wang, X. Yu, D. Lan, J. Zhao, S. Li, X. Tan, and Y. Yu, Coherent state transfer between superconducting qubits via stimulated Raman adiabatic passage, *Appl. Phys. Lett.* 118(10), 104003 (2021)
40. Z. Li, D. Li, M. Li, X. Yang, S. Song, Z. Han, Z. Yang, J. Chu, X. Tan, D. Lan, H. Yu, and Y. Yu, Quantum state transfer via multi-passage

Landau–Zener–Stückelberg interferometry in a three-qubit system, *Phys. Status Solidi B* 257(1), 1900459 (2020)
41. X. Li, Y. Ma, J. Han, T. Chen, Y. Xu, W. Cai, H. Wang, Y. P. Song, Z. Y. Xue, Z. Yin, and L. Sun, Perfect quantum state transfer in a superconducting qubit chain with parametrically tunable couplings, *Phys. Rev. Appl.* 10(5), 054009 (2018)
42. C. Zhang, T. L. Wang, Z. A. Zhao, X. Y. Yang, L. L. Guo, Z. L. Jia, P. Duan, and G. P. Guo, Fast and perfect state transfer in superconducting circuit with tunable coupler, *Chin. Phys. B* 32(11), 110305 (2023)
43. W. Zheng, J. Xu, Z. Wang, Y. Dong, D. Lan, X. Tan, and Y. Yu, Accelerated quantum adiabatic transfer in superconducting qubits, *Phys. Rev. Appl.* 18(4), 044014 (2022)
44. F. A. Roy, J. H. Romeiro, L. Koch, I. Tsitsilin, J. Schirk, N. J. Glaser, N. Bruckmoser, M. Singh, F. X. Haslbeck, G. B. P. Huber, G. Krylov, A. Marx, F. Pfeiffer, C. M. F. Schneider, C. Schweizer, F. Wallner, D. Bunch, L. Richard, L. Södergren, K. Liegener, M. Werninghaus, and S. Filipp, Parity-dependent state transfer for direct entanglement generation, *Nat. Commun.* 16(1), 2660 (2025)
45. J. Niu, L. Zhang, Y. Liu, J. Qiu, W. Huang, et al., Low-loss interconnects for modular superconducting quantum processors, arXiv: 2302.02751 (2023)
46. P. Kurpiers, P. Magnard, T. Walter, B. Royer, M. Pechal, J. Heinsoo, Y. Salathé, A. Akin, S. Storz, J. C. Besse, S. Gasparinetti, A. Blais, and A. Wallraff, Deterministic quantum state transfer and remote entanglement using microwave photons, *Nature* 558(7709), 264 (2018)
47. P. Magnard, S. Storz, P. Kurpiers, J. Schär, F. Marxer, J. Lütolf, T. Walter, J. C. Besse, M. Gabureac, K. Reuer, A. Akin, B. Royer, A. Blais, and A. Wallraff, Microwave quantum link between superconducting circuits housed in spatially separated cryogenic systems, *Phys. Rev. Lett.* 125(26), 260502 (2020)
48. H. S. Chang, Y. P. Zhong, A. Bienfait, M. H. Chou, C. R. Conner, É. Dumur, J. Grebel, G. A. Peairs, R. G. Povey, K. J. Satzinger, and A. N. Cleland, Remote entanglement via adiabatic passage using a tunably dissipative quantum communication system, *Phys. Rev. Lett.* 124(24), 240502 (2020)
49. Y. Zhong, H. S. Chang, A. Bienfait, É. Dumur, M. H. Chou, C. R. Conner, J. Grebel, R. G. Povey, H. Yan, D. I. Schuster, and A. N. Cleland, Deterministic multi-qubit entanglement in a quantum network, *Nature* 590(7847), 571 (2021)
50. A. Bienfait, K. J. Satzinger, Y. P. Zhong, H. S. Chang, M. H. Chou, C. R. Conner, É. Dumur, J. Grebel, G. A. Peairs, R. G. Povey, and A. N. Cleland, Phonon-mediated quantum state transfer and remote qubit entanglement, *Science* 364(6438), 368 (2019)
51. M. Baur, A. Fedorov, L. Steffen, S. Filipp, M. P. da Silva, and A. Wallraff, Benchmarking a quantum teleportation protocol in superconducting circuits using tomography and an entanglement witness, *Phys. Rev. Lett.* 108(4), 040502 (2012)
52. L. Steffen, Y. Salathe, M. Oppliger, P. Kurpiers, M. Baur, C. Lang, C. Eichler, G. Puebla-Hellmann, A. Fedorov, and A. Wallraff, Deterministic quantum teleportation with feed-forward in a solid state system, *Nature* 500(7462), 319 (2013)
53. J. Qiu, Y. Liu, L. Hu, Y. Wu, J. Niu, L. Zhang, W. Huang, Y. Chen, J. Li, S. Liu, Y. Zhong, L. Duan, and D. Yu, Deterministic quantum state and gate teleportation between distant superconducting chips, *Sci. Bull. (Beijing)* 70(3), 351 (2025)
54. R. J. Chapman, M. Santandrea, Z. Huang, G. Corrielli, A. Crespi, M. H. Yung, R. Osellame, and A. Peruzzo, Experimental perfect state transfer of an entangled photonic qubit, *Nat. Commun.* 7(1), 11339 (2016)
55. B. H. Huang, Y. H. Kang, Y. H. Chen, Z. C. Shi, J. Song, and Y. Xia, Quantum state transfer in spin chains via shortcuts to adiabaticity, *Phys. Rev. A* 97(1), 012333 (2018)
56. Y. H. Chen, Z. C. Shi, J. Song, and Y. Xia, Invariant-based inverse engineering for fluctuation transfer between membranes in an optomechanical cavity system, *Phys. Rev. A* 97(2), 023841 (2018)
57. J. X. Han, J. L. Wu, Z. H. Yuan, Y. J. Chen, Y. Xia, Y. Y. Jiang, and J. Song, Fast and controllable topological excitation transfers in hybrid magnon–photon systems, *Phys. Rev. Appl.* 21(1), 014057 (2024)
58. L. Zhou, Q. Xu, T. Feng, and X. Zhou, Experimental realization of a three-photon asymmetric maximally entangled state and its application to quantum state transfer, *Sci. Adv.* 10(25), eadj9251 (2024)
59. T. Liu, Z. F. Zheng, Y. Zhang, Y. L. Fang, and C. P. Yang, Transferring entangled states of photonic cat-state qubits in circuit QED, *Front. Phys. (Beijing)* 15(2), 21603 (2020)
60. Q. P. Su, H. Zhang, and C. P. Yang, Transferring quantum entangled states between multiple single-photon-state qubits and coherent-state qubits in circuit QED, *Front. Phys. (Beijing)* 16(6), 61501 (2021)
61. X. L. He, Z. F. Zheng, Y. Zhang, and C. P. Yang, One-step transfer of quantum information for a photonic cat-state qubit, *Quantum Inform. Process.* 19(3), 80 (2020)
62. J. Xu and T. Liu, Transfer of arbitrary quantum states between separated superconducting cavities via an ensemble of nitrogen–vacancy centers, *Results Phys.* 44, 106157 (2023)
63. Y. Wang, Q. P. Su, T. Liu, G. Q. Zhang, W. Feng, Y. Yu, and C. P. Yang, Long-distance transmission of arbitrary quantum states between spatially separated microwave cavities, *Opt. Express* 32(3), 4728 (2024)
64. G. F. Peñas, R. Puebla, and J. J. García-Ripoll, Multiplexed quantum state transfer in waveguides, *Phys. Rev. Res.* 6(3), 033294 (2024)
65. Y. Xu, D. Zhu, F. X. Sun, Q. He, and W. Zhang, Fast quantum state transfer and entanglement preparation in strongly coupled bosonic systems, *New J. Phys.* 25(11), 113015 (2023)
66. X. Leu, X. H. T. Nguyen, and J. Lee, Quantum state transfer of superposed multi-photon states via phonon-induced dynamic resonance in an optomechanical system, arXiv: 2501.01647 (2025)
67. S. Eshete, Quantum information transfer between optical

and microwave output modes via cavity magnonics, *J. Magn. Magn. Mater.* 549, 168987 (2022)

68. C. J. Axline, L. D. Burkhart, W. Pfaff, M. Zhang, K. Chou, P. Campagne-Ibarcq, P. Reinhold, L. Frunzio, S. M. Girvin, L. Jiang, M. H. Devoret, and R. J. Schoelkopf, On-demand quantum state transfer and entanglement between remote microwave cavity memories, *Nat. Phys.* 14(7), 705 (2018)
69. J. Grebel, H. Yan, M. H. Chou, G. Andersson, C. R. Conner, Y. J. Joshi, J. M. Miller, R. G. Povey, H. Qiao, X. Wu, and A. N. Cleland, Bidirectional multiphoton communication between remote superconducting nodes, *Phys. Rev. Lett.* 132(4), 047001 (2024)
70. N. Leung, Y. Lu, S. Chakram, R. K. Naik, N. Earnest, R. Ma, K. Jacobs, A. N. Cleland, and D. I. Schuster, Deterministic bidirectional communication and remote entanglement generation between superconducting qubits, *npj Quantum Inf.* 5, 18 (2019)
71. J. Zhou, M. Li, W. Wang, W. Cai, Z. Hua, Y. Xu, X. Pan, G. Xue, H. Zhang, Y. Song, H. Yu, C. L. Zou, and L. Sun, Quantum state transfer between superconducting cavities via exchange-free interactions, *Phys. Rev. Lett.* 133(22), 220801 (2024)
72. L. D. Burkhart, J. D. Teoh, Y. Zhang, C. J. Axline, L. Frunzio, M. H. Devoret, L. Jiang, S. M. Girvin, and R. J. Schoelkopf, Error-detected state transfer and entanglement in a superconducting quantum network, *PRX Quantum* 2(3), 030321 (2021)
73. L. N. Zheng, L. Qi, L. Y. Cheng, H. F. Wang, and S. Zhang, Defect-induced controllable quantum state transfer via a topologically protected channel in a flux qubit chain, *Phys. Rev. A* 102(1), 012606 (2020)
74. L. Y. Cheng, L. N. Zheng, R. X. Wu, H. F. Wang, and S. Zhang, Change-over switch for quantum states transfer with topological channels in a circuit-QED lattice, *Chin. Phys. B* 31(2), 020305 (2022)
75. J. Lu, L. Zhou, L. M. Kuang, and F. Nori, Single-photon router: Coherent control of multi-channel scattering for single photons with quantum interferences, *Phys. Rev. A* 89(1), 013805 (2014)
76. Y. Li, Z. Bao, Z. Wang, Y. Wu, J. Wang, J. Yang, H. Xiong, Y. Song, H. Zhang, and L. Duan, Quantum switch for itinerant microwave single photons with superconducting quantum circuits, *Phys. Rev. Appl.* 21(4), 044030 (2024)
77. X. Y. Zhang, Y. Yan, L. N. Zheng, Z. X. Zhang, L. N. Zhong, S. Zhang, and H. F. Wang, Topological phase and tunable quantum state transfer of Su–Schrieffer–Heeger chain with an embedded quantum ring, *Adv. Quantum Technol.* 7(8), 2400156 (2024)
78. W. Feng, Z. Y. Wei, G. Q. Zhang, J. Y. Li, J. X. Zhang, and C. P. Yang, Quantum routing based on chiral state transfer in arbitrary *N*-node networks, *Phys. Rev. A* 111(4), 042423 (2025)
79. M. Neeley, M. Ansmann, R. C. Bialczak, M. Hofheinz, N. Katz, E. Lucero, A. O'Connell, H. Wang, A. N. Cleland, and J. M. Martinis, Process tomography of quantum memory in a Josephson-phase qubit coupled to a two-level state, *Nat. Phys.* 4(7), 523 (2008)
80. G. Sun, X. Wen, B. Mao, J. Chen, Y. Yu, P. Wu, and S. Han, Tunable quantum beam splitters for coherent manipulation of a solid-state tripartite qubit system, *Nat. Commun.* 1(1), 51 (2010)
81. R. Barends, J. Kelly, A. Megrant, A. Veitia, D. Sank, E. Jeffrey, T. C. White, J. Mutus, A. G. Fowler, B. Campbell, Y. Chen, Z. Chen, B. Chiaro, A. Dunsworth, C. Neill, P. O'Malley, P. Roushan, A. Vainsencher, J. Wenner, A. N. Korotkov, A. N. Cleland, and J. M. Martinis, Super conducting quantum circuits at the surface code threshold for fault tolerance, *Nature* 508(7497), 500 (2014)
82. M. Sandberg, C. M. Wilson, F. Persson, T. Bauch, G. Johansson, V. Shumeiko, T. Duty, and P. Delsing, Tuning the field in a microwave resonator faster than the photon lifetime, *Appl. Phys. Lett.* 92(20), 203501 (2008)
83. Z. L. Wang, Y. P. Zhong, L. J. He, H. Wang, J. M. Martinis, A. N. Cleland, and Q. W. Xie, Quantum state characterization of a fast tunable superconducting resonator, *Appl. Phys. Lett.* 102(16), 163503 (2013)
84. J. Koch, T. M. Yu, J. Gambetta, A. A. Houck, D. I. Schuster, J. Majer, A. Blais, M. H. Devoret, S. M. Girvin, and R. J. Schoelkopf, Charge-insensitive qubit design derived from the Cooper pair box, *Phys. Rev. A* 76(4), 042319 (2007)
85. C. P. Yang and S. Han, Rotation gate for a three-level superconducting quantum interference device qubit with resonant interaction, *Phys. Rev. A* 74(4), 044302 (2006)
86. A. Anferov, S. P. Harvey, F. Wan, J. Simon, and D. I. Schuster, Superconducting qubits above 20 GHz operating over 200 mK, *PRX Quantum* 5(3), 030347 (2024)
87. P. Liu, R. Wang, J. N. Zhang, Y. Zhang, X. Cai, H. Xu, Z. Li, J. Han, X. Li, G. Xue, W. Liu, L. You, Y. Jin, and H. Yu, Performing $SU(d)$ operations and rudimentary algorithms in a superconducting transmon qudit for $d = 3$ and $d = 4$, *Phys. Rev. X* 13(2), 021028 (2023)
88. I. C. Hoi, C. M. Wilson, G. Johansson, T. Palomaki, B. Peropadre, and P. Delsing, Demon-stration of a single-photon router in the microwave regime, *Phys. Rev. Lett.* 107(7), 073601 (2011)
89. For a transmon qutrit, the $|g\rangle \leftrightarrow |f\rangle$ transition is much weaker than those of the $|g\rangle \leftrightarrow |e\rangle$ and $|e\rangle \leftrightarrow |f\rangle$ transitions. Thus, we have $\gamma_{fg}^{-1} \gg \gamma_{eg}^{-1}, \gamma_{fe}^{-1}$.
90. C. Rigetti, J. M. Gambetta, S. Poletto, B. L. T. Plourde, J. M. Chow, A. D. Corcoles, J. A. Smolin, S. T. Merkel, J. R. Rozen, G. A. Keefe, M. B. Rothwell, M. B. Ketchen, and M. Steffen, Superconducting qubit in waveguide cavity with coherence time approaching 0.1 ms, *Phys. Rev. B* 86, 100506(R) (2012)
91. M. J. Peterer, S. J. Bader, X. Jin, F. Yan, A. Kamal, T. J. Gudmundsen, P. J. Leek, T. P. Orlando, W. D. Oliver, and S. Gustavsson, Coherence and decay of higher energy levels of a superconducting transmon qubit, *Phys. Rev. Lett.* 114(1), 010501 (2015)
92. M. Pechal, L. Huthmacher, C. Eichler, S. Zeytinôglu, S. Abdumalikov, A. Berger, A. Wallraff, and S. Filipp, Microwave-controlled generation of shaped single photons in circuit quantum electrodynamics, *Phys. Rev. X* 4(4), 041010 (2014)
93. S. Zeytinoğlu, M. Pechal, S. Berger, A. Abdumalikov,

A. Wallraff, and S. Filipp, Microwave-induced amplitude- and phase-tunable qubit-resonator coupling in circuit quantum electrodynamics, *Phys. Rev. A* 91(4), 043846 (2015)

94. T. Noh, Z. Xiao, X. Y. Jin, K. Cicak, E. Doucet, J. Aumentado, L. C. G. Govia, L. Ranzani, A. Kamal, and R. W. Simmonds, Strong parametric dispersive shifts in a statically decoupled two-qubit cavity QED system, *Nat. Phys.* 19(10), 1445 (2023)
95. S. J. Bosman, M. F. Gely, V. Singh, A. Bruno, D. Bothner, and G. A. Steele, Multi-mode ultra-strong coupling in circuit quantum electrodynamics, *npj Quantum Inform.* 3, 46 (2017)
96. M. Baur, S. Filipp, R. Bianchetti, J. M. Fink, M. Göppl, L. Steffen, P. J. Leek, A. Blais, and A. Wallraff, Measurement of Autler–Townes and Mollow transitions in a strongly driven superconducting qubit, *Phys. Rev. Lett.* 102(24), 243602 (2009)
97. W. Woods, G. Calusine, A. Melville, A. Sevi, E. Golden, D. K. Kim, D. Rosenberg, J. L. Yoder, and W. D. Oliver, Determining interface dielectric losses in superconducting coplanar-waveguide resonators, *Phys. Rev. Appl.* 12(1), 014012 (2019)
98. A. Melville, G. Calusine, W. Woods, K. Serniak, E. Golden, B. M. Niedzielski, D. K. Kim, A. Sevi, J. L. Yoder, E. A. Dauler, and W. D. Oliver, Comparison of dielectric loss in titanium nitride and aluminum superconducting resonators, *Appl. Phys. Lett.* 117(12), 124004 (2020)
99. M. H. Amini, A. Mallahzadeh, and A. Ghasemi, Crosstalk between superconducting microstrip transmission lines, *IEEE Trans. Electromagn. Compat.* 65(5), 1529 (2023)
100. C. P. Yang, Q. P. Su, and S. Y. Han, Generation of Greenberger–Horne–Zeilinger entangled states of photons in multiple cavities via a superconducting qutrit or an atom through resonant interaction, *Phys. Rev. A* 86(2), 022329 (2012)
101. V. A. Sevriuk, K. Y. Tan, E. Hyyppä, M. Silveri, M. Partanen, M. Jenei, S. Masuda, J. Goetz, V. Vesterinen, L. Grönberg, and M. Möttönen, Fast control of dissipation in a superconducting resonator, *Appl. Phys. Lett.* 115(8), 082601 (2019)
102. M. Jerger, F. Motzoi, Y. Gao, C. Dickel, L. Buchmann, A. Bengtsson, G. Tancredi, C. W. Warren, J. Bylander, D. DiVincenzo, R. Barends, and P. A. Bushev, Dispersive qubit readout with intrinsic resonator reset, arXiv: 2406.04891, (2024)